Article

Not peer-reviewed version

Enhanced Fracture Toughness of Dental Zirconia through Nb Incorporation into the Surface

Seiji Ban * and Yuta Yasuoka

Posted Date: 2 August 2024

doi: 10.20944/preprints202408.0063.v1

Keywords: zirconia; fracture toughness; niobium; surface modification; thermal expansion

 doi:10.20944/preprints202408.0063.v1

Article

Enhanced Fracture Toughness of Dental Zirconia through Nb Incorporation into the Surface

Seiji Ban [1,*] and Yuta Yasuoka [2]

[1] Department of Dental Materials Science, School of Dentistry, Aichi Gakuin University
[2] KCM Corporation; yasuoka_yuta@kyoritsu-kcm.co.jp
* Correspondence: sban@g.agu.ac.jp; Tel.: +81-052-751-2561

Abstract: Background: Our previous study revealed that the addition of pentavalent cations, such as niobium (Nb), to zirconia stabilized with trivalent cations, such as yttrium (Y), increased fracture toughness. However, the coefficient of thermal expansion (CTE) and opacity also increased undesirably. Thus, a novel surface treatment is required to enhance fracture toughness without changing the CTE and the translucency. Methods: The surfaces of pre-sintered 3-mol% yttria-stabilized tetragonal zirconia polycrystal (3Y-TZP) and 4.2-mol% yttria-stabilized partially stabilized zirconia (4.2Y-PSZ) were treated with an Nb sol solution containing Nb_2O_5 nanoparticles. After drying and final sintering, a surface layer with high Nb content formed to a depth of approximately 1 mm. Results: Nb was equivalent to that of the bulk uniformly containing 1 mol% Nb_2O_5. The tetragonality of tetragonal zirconia near the surface increased with the addition of Nb, leading to improve fracture toughness in the surface layer and enhancing the fracture toughness of the entire specimen. However, the CTE and the translucency remained unchanged. Conclusions: The addition of pentavalent cations such as Nb, confined to the surface vicinity, improved fracture toughness without affecting the CTE and the translucency. By selectively adding Nb to the surface of weak parts of zirconia prosthesis, the overall strength can be improved, making it possible to produce highly reliable dental restorations.

Keywords: zirconia; fracture toughness; niobium; surface modification; thermal expansion

1. Introduction

Dental zirconia has evolved significantly and is now widely used as an aesthetic dental restorative material. Yttria (Y_2O_3) is commonly used as a stabilizer to enhance strength and toughness. When the yttria content ranges from 3 to 8 mol%, both tetragonal and cubic phases coexist at room temperature, forming partially stabilized zirconia (PSZ). At around 3 mol%, the tetragonal phases approach 100% at room temperature, forming tetragonal zirconia polycrystal (TZP). Initially, 3 mol% yttria-stabilized TZP (3Y-TZP) was introduced as a core material to replace metal in dental applications. However, due to its low translucency, the surface of 3Y-TZP must be veneered with feldspathic porcelain to enhance its appearance. To exploit the high strength of zirconia without porcelain veneering, high-translucency 4 mol% and 5 mol% yttria stabilized PSZ (4Y-PSZ and 5Y-PSZ) have been developed for monolithic zirconia prostheses [1]. Increasing the translucency of PSZ can be achieved by increasing the stabilizer content, such as yttria, though this may reduce the strength of zirconia [2]. Additionally, ultra-high translucency zirconia (UHTZ) has been developed using novel manufacturing techniques to achieve particularly high translucency [3]. Consequently, numerous types of zirconia are available for dental treatment, classified mainly into three categories: single colors with different yttria contents, single composition multilayer types (uniform composition with different colored multilayers), and mixed composition multilayer types (multilayers with different compositions and coloring). Based on yttria content and multilayer construction, these can be classified into 13 types [4].

 doi:10.20944/preprints202408.0063.v1

In our previous study, forty-four types of zirconia were prepared by combining yttrium (Y), ytterbium (Yb), niobium (Nb), and tantalum (Ta) oxide as stabilizers, and were evaluated them for fracture toughness and opacity [5]. The results indicated that adding trivalent cations Y and/or Yb reduced fracture toughness and opacity, whereas adding pentavalent cations Nb and/or Ta to ZrO_2 stabilized with trivalent cations increased both properties. There was no significant difference in the effects between Y and Yb, or between Nb and Ta. Furthermore, these effects were similar for additions to 3Y-TZP and 4Y-PSZ.

However, while the addition of pentavalent cations increased the fracture toughness of zirconia, it also increased the coefficient of thermal expansion (CTE) and the opacity. As the opacity increases, indicating decrease in translucency, it becomes necessary to improve aesthetics by applying porcelain veneering or glazing to the surface. Veneer porcelains and glazing materials for zirconia are designed to match the original CTE of zirconia, and changes in CTE can render these coating unusable. Therefore, maintaining a constant CTE and translucency is crucial. In this study, we developed a novel surface treatment using Nb sol for zirconia to enhance fracture toughness while sustaining the original CTE and translucency. This approach utilizes the novel technique to address the inherent weaknesses of zirconia, particularly at stress concentration points, thereby producing highly reliable dental restorations.

2. Materials and Methods

2.1. Preparation

Table 1 displays the chemical composition of four zirconia powders prepared by combining yttrium and niobium oxide as stabilizers, and two Nb sol specimens.

Table 1. Chemical composition of specimens used in this study.

Code	Composition (mol%)		
	ZrO_2	Y_2O_3	Nb_2O_5
3Y-TZP	97.0	3.0	-
4.2Y-PSZ	95.8	4.2	-
3Y-1 mol% Nb_2O_5	96.03	2.97	1.0
4.2Y-1 mol% Nb_2O_5	94.842	4.158	1.0

Zirconia powders (KCM Corporation, Nagoya, Japan) containing 3 mol% and 4.2 mol% yttrium oxide (Y_2O_3) (3Y-TZP and 4.2Y-PSZ) were prepared as our previous method [5]. Additionally, two materials (3Y-1 mol% Nb_2O_5 and 4.2Y-1 mol% Nb_2O_5) were prepared by mixing Nb_2O_5 with 3Y-TZP and 4.2Y-PSZ powders to achieve a 1 mol% Nb_2O_5 concentration in the entire mixture. After mixing, 15 g of these powders were placed into a mold with a bottom surface area of 50 mm by 15 mm, and a preformed body was created under a pressure of 20 MPa.

For thermal expansion and opacity specimen preparation, 1.5 g and 1.7 g of these powders were filled into molds with diameters of 7 mm and 20 mm, respectively, and subjected to a pressure of 0.78 MPa to produce preformed bodies. After removing these preforms from the molds, they were subjected to CIP molding at a pressure of 196 MPa to produce molded bodies. These molded bodies were calcined at 1000 °C for 30 minutes to obtain pre-sintered bodies. The pre-sintered bodies were then fired at 1450 °C for 2 hours to obtain sintered bodies.

The sintered body intended for general measurement had a rectangular shape with dimensions of 40 mm in length, 11.5 mm in width, and 10 mm in height. The sintered body for thermal expansion measurements had a cylindrical shape with a diameter of 5.5 mm and a height of 10 mm. The sintered body for opacity measurements had a disc shape with a diameter of 14.5 mm and a thickness of 1.6 mm, and the thickness was adjusted to 1.5 mm by mirror polishing.

 doi:10.20944/preprints202408.0063.v1

2.2. Nb Incorporation into Zirconia Surface

For the preparation of 3Y- and 4.2Y-Nb sol, the pre-sintered bodies of 3Y-TZP and 4.2Y-PSZ were soaked in a Nb_2O_5 sol (Biral Nb-G6000, Taki Chemical Co., Ltd., Kakogawa, Hyogo, Japan) for 24 hours for the specimen other than those for thermal expansion, and for 4.5 hours for thermal expansion specimen, then dried at 120 °C for 16 hours.

After drying, the Nb incorporated-pre-sintered specimens were sintered at 1450 °C for 2 hours to obtain the final sintered body. The Nb-incorporated sintered-body was cut perpendicular to its long side (40 mm side) to prepare specimens for fracture toughness and Nb concentration analysis, with a cut surface measuring 11.5 mm by 5.6 mm at the midpoint of the long side using a diamond cutter. The cut surface was mirror-polished with a diamond paste.

2.3. Fracture Toughness

Indentation Fracture (IF) method was employed to determine the depth profile of fracture toughness in this study. According to the IF method specified in JIS R 1607: 2015, "Testing methods for fracture toughness of fine ceramics at room temperature", fracture toughness values were determined using a Vickers hardness tester (MV-1, Matsuzawa Co., Ltd., Akita, Japan) for each specimen according to the following equation:

$$K_{Ic} = 0.18(E/Hv)^{0.5}(P/c^{1.5}), \quad (1)$$

where K_{IC} is the fracture toughness (Pa√m), E is the modulus of elasticity (Pa) (206 GPa was employed in this study), H_V is Vickers hardness (Pa) [$Hv = 0.1891P/(2a)^2$], P is the indentation load (N) (98 N was employed in this study), c is half of the average crack length (m), a is half of the average diagonal length of the indenter (m). Measurements were performed on the surface of six types of sintered bodies and the section of 3Y-Nb sol sintered body.

2.4. Thermal Expansion

The average linear expansion coefficient from 25 °C to 500 °C was measured using a thermomechanical analyzer (TMA4000SA, Netzsch-Geratebau GmbH, Selb, Bayern, Germany). The measurement was performed according to JIS R 1618 under the following conditions: load of 20 g, the heating rate of 5 K/min, and air atmosphere.

2.5. Opacity

Using a spectrophotometer (CM-3700d, Konica Minolta Co., Ltd.), the reflectance (R_1 and R_0) of a disc-shaped specimen with a thickness of 1.5 mm were measured against the black and white background, respectively. The opacity (%) is automatically calculated from the measurement results according to the formula:

$$\text{Opacity (\%)} = R_1/R_0 \times 100 \quad (2)$$

When measuring the reflectance from 360 to 740 nm, a calibration plate (CM-A90) and a zero calibration box (CM-A94) was used as a white and a black background, respectively. Measurement geometry was set to the SCI reflectance, 8 mm measurement diameter, 100% Full UV condition, 10° viewing angle, and D65 light source. Measurements were repeated 3 times for each specimen, and the average value over the 3 measurements was calculated.

2.6. Nb Concentration Analysis

After mirror-finishing the cut surface of the 3Y-Nb sol, the cut surface was analyzed using a scanning electron microscope with wavelength dispersive X-ray spectroscopy (SEM-WDX) (JXA-iHP200F Hyper Probe, JEOL Ltd., Tokyo, Japan). Two methods were used to measure the Nb concentration distribution: a method using the results of the Nb characteristic X-ray intensity from the elemental mapping image, and a method using quantitative analysis results.

 doi:10.20944/preprints202408.0063.v1

For Nb elemental mapping, a WDS PET detector was used under the following conditions: accelerating voltage of 15.0 kV, irradiation current of 5.0 x 10^{-8} A, collection time of 10 msec, and pixel size of 2.5 μm (at 100x magnification). Elemental mapping was performed along the short side direction of the cut surface, passing through the center. Six mapping images of Nb concentration and six secondary electron images (SEI) were combined into a single image of the total cut surface.

Quantitative analysis of Nb in the 3Y-Nb sol sintered body and the 3Y-1 mol% Nb_2O_5 was conducted at positions of 0 mm, ±0.5 mm, ±1.5 mm, ±2.5 mm, and ±2.7 mm from the center. This analysis was performed using Nb WDS PET detector, with an accelerating voltage of 15.0 kV, irradiation current of 5.0×10^{-8} A, and a collection time of 500 msec. The obtained Nb analytical value was normalized by subtracting the background and using the average Nb analytical value of 3Y-1.0 mol% Nb_2O_5 as 1 mol% Nb_2O_5.

2.7. X-ray Diffractometry

X-ray diffraction patterns (XRD) of the polished specimens were measured using an X-ray diffractometer (Ultima IV, Rigaku Corporation, Tokyo, Japan) under conditions of at 40 kV and 40 mA. Scans were conducted between 72° and 76° in 2θ at 0.04°/min using Cu Ka radiation. The lattice constants of the tetragonal *c*-axis and *a*-axis were derived from the (004) and (400) peak positions around 73° and 74.5°, respectively, using analysis software (PDXL2). The tetragonal *c*/*a* axis lattice constant ratios were calculated from these values.

3. Results

3.1. Fracture Toughness, Thermal Expansion and Opacity

The fracture toughness of the sintered bodies of 3Y-TZP and 4.2Y-PSZ coated with Nb sol and containing 1 mol% Nb_2O_5 were higher than those without Nb_2O_5 (Figure 1).

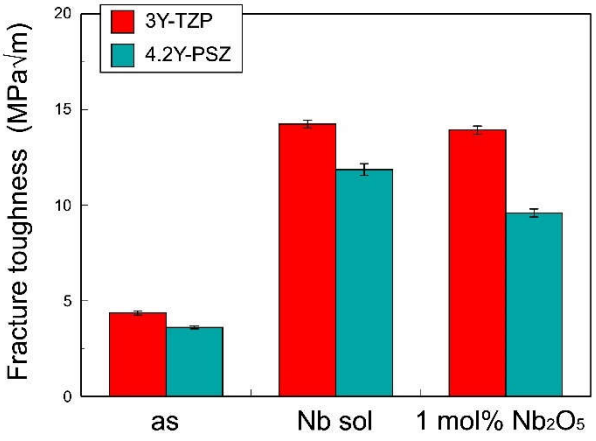

Figure 1. Fracture toughness of the surface of 3Y-TZP, 3Y-Nb sol, 3Y-1 mol% Nb_2O_5, 4.2Y-PSZ, 4.2Y-Nb sol, and 4.2Y-1 mol% Nb_2O_5.

Conversely, the coefficient of thermal expansion (CTE) and the opacity of 3Y-TZP and 4.2Y-PSZ containing 1 mol% Nb_2O_5 were larger than those without Nb_2O_5, while the CTE and the opacity of 3Y-TZP and 4.2Y-PSZ coated with Nb sol were nearly the same as those without Nb_2O_5 (Figures 2 and 3).

 doi:10.20944/preprints202408.0063.v1

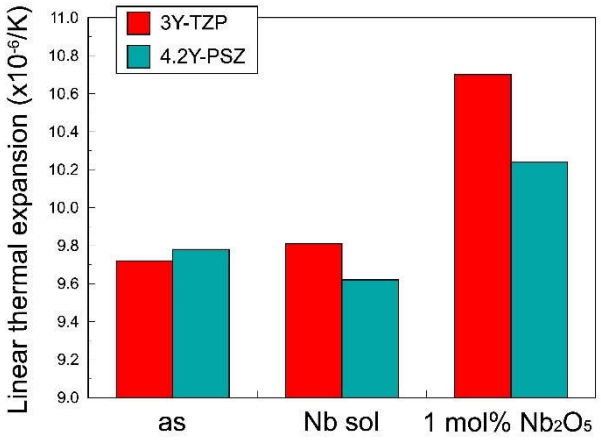

Figure 2. Coefficient of linear thermal expansion of 3Y-TZP, 3Y-Nb sol, 3Y-1 mol% Nb_2O_5, 4.2Y-PSZ, 4.2Y-Nb sol, and 4.2Y-1 mol% Nb_2O_5.

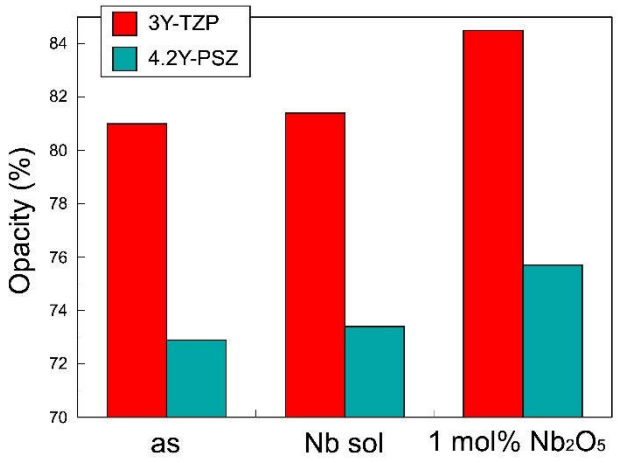

Figure 3. Coefficient of opacity of 3Y-TZP, 3Y-Nb sol, 3Y-1 mol% Nb_2O_5, 4.2Y-PSZ, 4.2Y-Nb sol, and 4.2Y-1 mol% Nb_2O_5.

These results suggest that Nb incorporation into the zirconia surface enhances the fracture toughness similar to zirconia containing 1 mol% Nb homogeneously, while suppressing thermal expansion and opacity.

3.2. Distribution of Nb

In the Nb mapping image of the sintered 3Y-Nb sol section (Figure 4), relatively bright areas indicating high Nb concentration was observed on both sides at about 1 mm depth from the surface, and relatively dark areas indicating low Nb concentration were observed in the middle of the section.

Preprints.org (www.preprints.org) | NOT PEER-REVIEWED | Posted: 2 August 2024 doi:10.20944/preprints202408.0063.v1

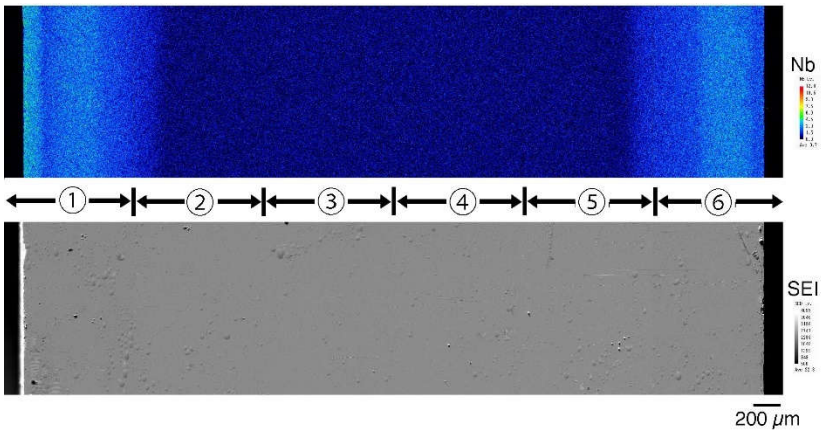

Figure 4. Nb concentration map (upper) and SEI (lower) of the section of sintered 3Y-Nb sol. Six mapping images of Nb concentration and six SEI were united into each image of the total cut surface, respectively. The relatively bright area indicates high Nb concentration, and relatively dark area indicates low Nb concentration.

Qualitative analysis results of Nb_2O_5 (Figure 5) showed that the Nb_2O_5 concentration in the 3Y-1 mol% Nb_2O_5 section was consistently about 1 mol% across all areas, whereas in the 3Y-Nb sol section, the Nb_2O_5 concentration dramatically varied with the distance from the surface. Almost no Nb_2O_5 was detected in the middle area, with Nb_2O_5 segregated on the surface layer at a depth of 1 mm.

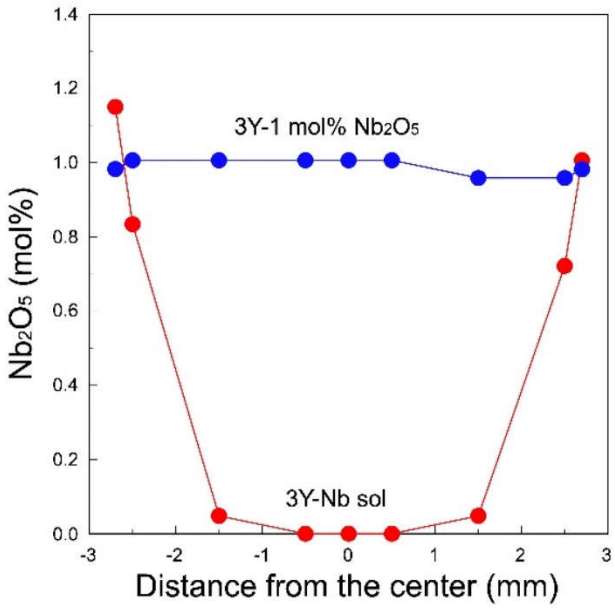

Figure 5. Analyzed Nb_2O_5 content of the section of sintered 3Y-1 mol% Nb_2O_5 and sintered 3Y-Nb sol. The horizontal axis indicates the distance from the center of the section, and the vertical axis indicates the converted Nb_2O_5 concentration.

About 1 mol% Nb_2O_5 was observed in the outermost surface area. 4.2Y-Nb sol showed similar Nb distribution to that of 3Y-Nb sol as not shown in figure.

3.3. Change in Crystal Lattice

XRD patterns of the sintered 3Y-Nb sol section varied with the distance from the center (Figure 6).

 doi:10.20944/preprints202408.0063.v1

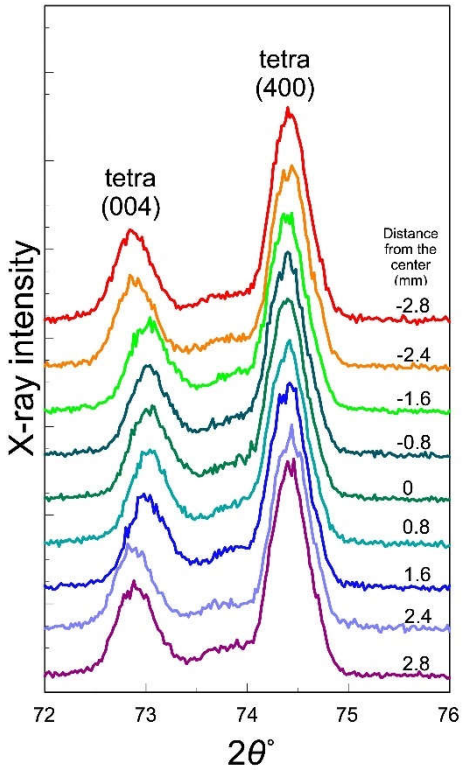

Figure 6. XRD patterns of the section of sintered 3Y-Nb sol.

The diffraction peak around 74.3° in 2θ is assigned to (400) of tetragonal zirconia and the peak at 72.8-73.0° in 2θ is assigned to (004) of tetragonal zirconia. The peak position of (400) was consistent, whereas the peak position of (004) changed with the distance from the center. The peak positions at -1.6 to 1.6 mm from the center were around 73° in 2θ, while the peak position at ±2.4 and ±2.8 mm from the center, indicating vicinity of surface, were around 72.8° in 2θ.

Lattice constants of *a*- and *c*-axis of the sintered 3Y-Nb sol section were derived from the (400) and (004) peak positions in their XRD patterns (Figure 7).

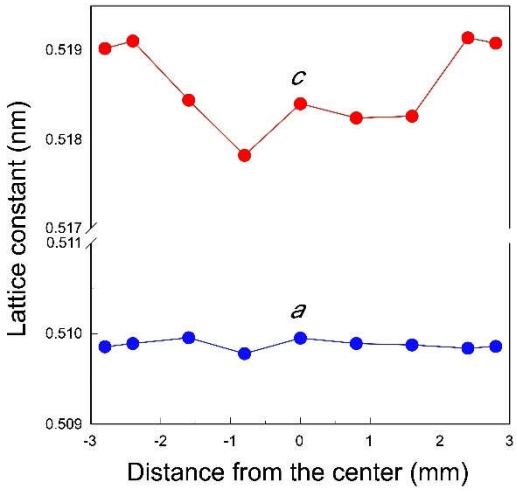

Figure 7. Distribution of lattice constant of *a*- and *c*-axis of the section of sintered 3Y-Nb sol.

Lattice constants of the *a*-axis were almost constant as 0.510 nm, whereas those of c-axis varied with the distance from the center. Lattice constants of the *c*-axis at -1.6 to 1.6 mm from the center were about 0.518 nm, while those at ±2.4 and ±2.8 mm from the center were about 0.519 nm.

Lattice constant ratios (*c*/*a*) of the sintered 3Y-Nb sol section were derived from these data (Figure 8). The tetragonal *c*/*a* ratio, indicating the stability and the crystallinity of the tetragonal

 doi:10.20944/preprints202408.0063.v1

zirconia, was about 1.0158-1,0165 at -1.6 to 1.6 mm from the center, and about 1.018 at ±2.4 and ±2.8 mm from the center.

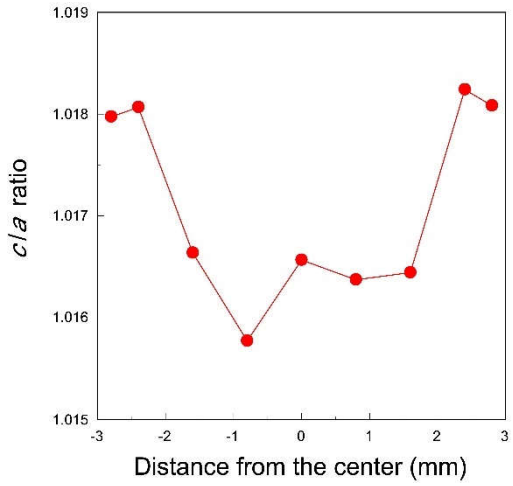

Figure 8. Distribution of lattice constant ratio *c*/*a* of the section of sintered 3Y-Nb sol.

3.4. Distribution of Fracture Toughness

Fracture toughness of the sintered 3Y-Nb sol section varied with the distance from the center (Figure 9).

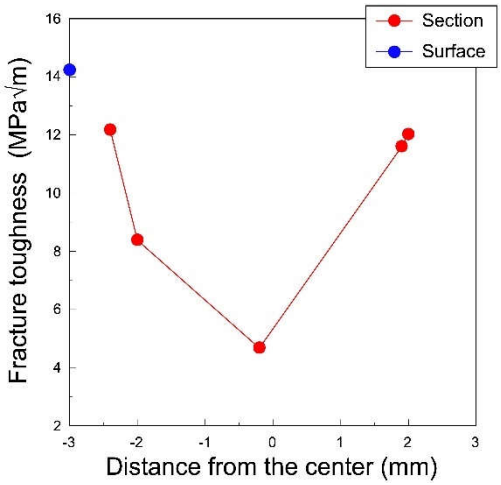

Figure 9. Distribution of fracture toughness of the section and the surface of sintered 3Y-Nb sol.

The fracture toughness at center showed the minimum value of 5 MPa√m, increasing to about 12 MPa√m closer to the surface. The fracture toughness on the surface was approximately 14.2 MPa√m.

4. Discussion

Our previous study revealed that addition of pentavalent cations such as Nb and Ta to ZrO_2 stabilized with trivalent cations such as Y and Yb increased fracture toughness [5]. Furthermore, the fracture toughness increased with the tetragonality (*c*/*a* ratio). If the *c*/*a* ratio is 1, the crystal phase is cubic. When pentavalent Nb and/or Ta are co-doped with Y and/or Yb, these cations stabilized the tetragonal structure and increase tetragonality by removing oxygen vacancies, forming the charge compensating pair such as Y-Nb, Yb-Nb, Y-Ta, and Yb-Ta [6–9]. Kim et al. demonstrated that the reduction of oxygen vacancies is responsible for the increased fracture toughness [6].

 doi:10.20944/preprints202408.0063.v1

In addition to fracture toughness, thermal expansion increased with tetragonality [10,11]. Thermal expansion in the c-axis direction was greater than that in the a-axis direction across the entire composition range. This anisotropic thermal expansion behavior is attributed to the four-fold coordination of Nb^{5+} with oxygen ions in tetragonal ZrO_2 solid solutions [12].

As mentioned above, while an increase in fracture toughness is desirable, an increase in the coefficient of thermal expansion (CTE) is not. To achieve the objective of increasing fracture toughness without altering the CTE, Nb was applied solely to the surface. This approach resulted in an increase in fracture toughness for the entire specimen without a change in CTE.

To selectively add Nb to the surface, a method involving the application or immersion of the surface in a compound containing Nb was considered. Although various compounds were tested, a high concentration of Nb could not be achieve on the surface using ionic solutions such as Nb chloride or Nb nitrate. The objective was only met when Nb sol was applied or used for immersion. This sol is a water-based inorganic coating material composed of 6.0-6.4 wt% Nb_2O_5 nanoparticles, 0.2-0.7 wt% NH_3, and the remainder being water. After drying at 60°C for 16 hours, nanosized Nb_2O_5 particles (less than 5 nm) agglomerated (Figure 10, left).

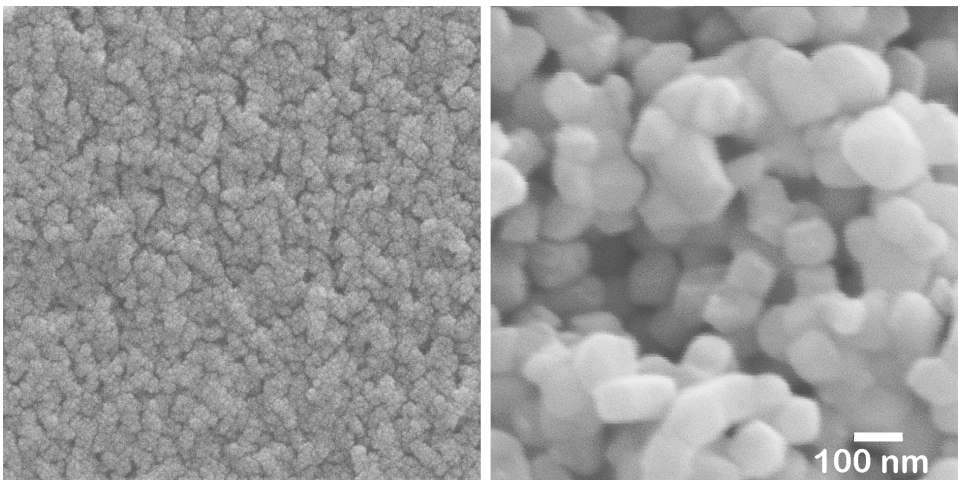

Figure 10. SEI of dried Nb-sol (left) and pre-sintered body (right).

These nanoparticles in the sol are significantly smaller than the pore size of pre-sintered zirconia (Figure 10, right). Therefore, the sol can easily penetrate to a depth of approximately 1 mm from the surface but not deeper. After final firing, a surface layer with high Nb content was formed to a depth of about 1 mm, as shown in Figures 4 and 5. The concentration of surface segregated Nb was equivalent to that of the bulk uniformly containing 1 mol% Nb_2O_5. Consequently, tetragonality increased only in the surface layer (Figure 8), and the fracture toughness also increased in this layer (Figure 9). This surface segregation was sufficient to enhance the fracture toughness of the entire body without increasing thermal expansion or decreasing translucency. The depth of segregation can be controlled by adjusting the sol concentration and the immersion time.

The effect of surface treatment on zirconia can be explained by the phenomenon caused by the formation of monoclinic crystals within tetragonal crystals. For example, sandblasting increases surface roughness, but the formation of monoclinic crystals generates compressive stress on the surface, improving bending strength [13–16]. On the other hand, it has been reported that when the amounts of monoclinic crystal formed on the surface becomes too large due to low temperature degradation, cracks occur and the strength decreases [16,17]. Thus, changes in the surface condition of zirconia affect the overall strength [18]. In this way, although the change is only on the surface, it convincingly results in an improvement in the overall strength. However, the CTE is independent of changes only on the surface; it is necessary to alter the material properties of the entire bulk.

The translucency of zirconia shows the same behavior. Our previous study demonstrated that the addition of Nb increases the opacity, i.e., reduces the translucency [5]. Again, when Nb is added only to the surface, the overall translucency is hardly affected. Therefore, the addition of pentavalent

 doi:10.20944/preprints202408.0063.v1

cations such as Nb, limited to the surface vicinity, improved fracture toughness without affecting the CTE and the translucency.

Even if it is made of zirconia, the joints of dental bridges where stress is likely to concentrate and the margins of dental crowns where the thickness is thin are prone to fracture. Adding Nb to the surface of weak parts of zirconia prosthesis can significantly enhance the overall strength and reliability of dental restorations. This approach leverages the beneficial properties of Nb addition to address the inherent weaknesses of zirconia, particularly at stress concentration points.

5. Conclusions

The surfaces of pre-sintered 3Y-TZP and 4.2Y-PSZ were treated with an Nb sol solution containing Nb_2O_5 nanoparticles. After drying and final sintering, a surface layer with high Nb content formed to a depth of approximately 1 mm. The concentration of surface-segregated Nb was equivalent to that of the bulk uniformly containing 1 mol% Nb_2O_5. The tetragonality of tetragonal zirconia in the surface vicinity increased with the addition of Nb. leading to improve fracture toughness in the surface layer and enhancing the fracture toughness of the entire specimen. However, the CTE and the translucency were independent of changes limited on the surface. Therefore, the addition of pentavalent cations such as Nb, confined to the surface vicinity, improved fracture toughness without affecting the CTE and the translucency. By selectively adding Nb to the surface of weak parts of zirconia prosthesis, the overall strength can be improved, making it possible to produce highly reliable dental restorations.

Author Contributions: Conceptualization, S.B. and Y.Y.; Data curation, Y.Y; Formal analysis, Y.Y.; Investigation, Y.Y.; Visualization, S.B.; Writing—original draft, S.B.; Writing—review and editing, S.B. and Y.Y. All authors have read and agreed to the published version of the manuscript.

Funding: This research received no external funding.

Institutional Review Board Statement: Not applicable.

Informed Consent Statement: Not applicable.

Data Availability Statement: Not applicable.

Acknowledgments: The authors would like to thank Hiroshi Tenjikukatsura, KCM Corporation, for allowing us to use the preparation equipment and the measurement devices.

Conflicts of Interest: The authors declare no conflict of interest.

References

1. Zhang, Y.; Lawn, B.R. Novel zirconia materials in dentistry. *J. Dent. Res.* **2018**, 97, 140–147.
2. Pekkan, G.; Pekkan, K.; Bayindir, B.Ç.; Ozcan, M.; Karasu, B. Factors affecting the translucency of monolithic zirconia ceramics: A review from materials science perspective. *Dent. Mater. J.* **2020**, 39, 1–8.
3. Ban, S. Development and characterization of ultra-high translucent zirconia using new manufacturing technology. *Dent. Mater. J.* **2023**, 42, 1-10.
4. Ban, S. Classification and properties of dental zirconia as implant fixtures and superstructures. *Materials* **2021**, 14, 4879.
5. Ban, S.; Yasuoka, Y.; Sugiyama, T.; Matsuura, Y. Translucent and highly toughened zirconia suitable for dental restorations. *Prosthesis* **2023**, 5, 60–72.
6. Kim, D.-J.; Jung, H.-J.; Jang, J.-W.; Lee, H.-L. Fracture toughness, ionic conductivity, and low-temperature phase stability of tetragonal codoped with yttria and niobium oxide. *J. Am. Ceram. Soc.* **1998**, 81, 2309–2314.
7. Kim, D.-J.; Tien, T.-Y. Phase stability and physical properties of cubic and tetragonal ZrO_2 in the system ZrO_2-Y_2O_3-Ta_2O_5. *J. Am. Ceram. Soc.* **1991**, 74, 3061–3065.
8. Kim, D.-J. Effect of Ta_2O_5, Nb_2O_5, and HfO_2 alloying on the transformability of Y_2O_3-stabilized tetragonal ZrO_2. *J. Am. Ceram. Soc.* **1990**, 73, 115–120.
9. Li, P.; Chen, I.-W.; Penner-Hahn, J.E. Effect of dopants on zirconia stabilization-An X-ray absorption study: III, Charge- compensating dopants. *J. Am. Ceram. Soc.* **1994**, 77, 1289–1294.
10. Schubert, H. Anisotropic thermal expansion coefficients of Y_2O_3-stabilized tetragonal zirconia. *J. Am. Ceram. Soc.* **1986**, 69, 270–271.
11. Shcu, T.-S. Anisotropic thermal expansion of tetragonal zirconia polycrystals. *J. Am. Ceram. Soc.* **1993**, 76, 1772–1776.

 doi:10.20944/preprints202408.0063.v1

12. Kim, D.-J.; Becher, P.F.; Hubbard, C.R. Effect of Nb_2O_5 alloying on thermal expansion anisotropy of 12 mol% Y_2O_3-stabilized tetragonal ZrO_2. *J. Am. Ceram. Soc.* **1993**, 76, 2904–2908.
13. Kosmac, T.; Oblak, C.; Jevnikar, P.; Funduk, N.; Marion, L. The effect of surface grinding and sandblasting on flexural strength and reliability of Y-TZP zirconia ceramic. *Dent. Mater.* **1999**, 15, 426-433.
14. Sato, H.; Yamada, K.; Pizzotti, G.; Nawa, M.; Ban, S. Mechanical properties of dental zirconia ceramics changed with sandblasting and heat treatment. *Dent. Mater. J.* **2008**, 27, 408–414.
15. Ban, S.; Sato, H.; Suehiro, Y.; Nakanishi, H.; Nawa, M. Biaxial flexure strength and low temperature degradation of Ce-TZP/Al_2O_3 nanocomposite and Y-TZP as dental restoratives. *J. Biomed. Mater. Res. B Appl. Biomater.* **2008**, 87, 492–498.
16. Ban, S.; Suehiro, Y.; Nakanishi, H.; Nawa, M. Fracture toughness of dental zirconia before and after autoclaving. *J. Ceram. Soc. Japan* **2010**, 118, 406-409.
17. Ban, S. Chemical durability of high translucent dental zirconia. *Dent. Mater. J.* **2020**, 39, 12–23.
18. Casucci, A.; Osorio, E.; Osorio, R.; Monticelli, F.; Toledano, M.; Mazzitelli, C.; Ferrari, M. Influence of different surface treatments on surface zirconia frameworks. *J. Dent.* **2009**, 37, 891-897.